10304 *Inorg. Chem.* **2009**, *48*, 10304–10311
DOI: 10.1021/ic901613s

Inorganic Chemistry
Article

Mercury(II) Recognition and Fluorescence Imaging *in Vitro* through a 3D-Complexation Structure

Mei-Lin Ho,*,† Kew-Yu Chen,‡ Gene-Hsiang Lee,‡ Yu-Chun Chen,‡ Chih-Chieh Wang,† Jyh-Fu Lee,§ Wen-Chun Chung,† and Pi-Tai Chou*,‡

†*Department of Chemistry, Soochow University, Taipei, Taiwan,* ‡*Department of Chemistry, National Taiwan University, Taipei, Taiwan, and* §*National Synchrotron Radiation Research Center, Hsinchu 300, Taiwan*

Received August 12, 2009

8,8′-(1,4,10,13-Tetrathia-7,16-diazacyclooctadecane-7,16-diyl)-bis(methylene)diquinolin-7-ol (**TTBQ**) was synthesized and proved to selectively recognize Hg^{2+}, forming a Hg^{2+}/**TTBQ** complex with an association constant (K_a) as large as $\sim 1.3 \times 10^4 \pm 520\ M^{-1}$ in aqueous solution. Single crystals of **TTBQ** and a **TTBQ**-Hg^{2+} complex have also been successfully grown, in which the latter unambiguously revealed a cagelike configuration consisting of thiol-crown and dual 7-hydroxyquinoline moieties to firmly trap Hg^{2+}. This 3D-complexation structure accounts for ~25-fold luminescence enhancement and a detection limit of sub-μM in water for sensing Hg^{2+}. Great selectivity toward Hg^{2+} has been exhibited over alkali- and alkaline-earth metal ions, first-row transition-metal ions, and other cations studied. This chemosensor is particularly suited for the detection of Hg^{2+} in a pH range of 5.5 to 7.5. This, in combination with its fine biocompatibility, leads to the success toward *in vitro* mercury recognition based on fluorescence imaging.

1. Introduction

Toxic and hazardous metal ions are detrimental to human life. Among these categories, Hg^{2+} is considered to be one of the most serious environmental and health threats. To date, considerable effort has been made to develop molecular sensing or recognition systems for the selective detection of Hg^{2+}.[1] However, most of the detection methods display one or more drawbacks in terms of actual applicability.[2] These include matrix interference and cross-sensitivities toward/from other metal ions (e.g., Cu^{2+}, Pb^{2+} ions), slow response to Hg^{2+}, the lack of water solubility, synthetic difficulties, and fluorescence quenching upon Hg^{2+} coordination via enhanced spin−orbit coupling, energy, or electron transfer. Nevertheless, among the numerous methodologies developed, the spectroscopic technique with Hg^{2+}-responsive chemosensors offers a promising and appealing approach for simple and rapid tracking of Hg^{2+}.[3]

In our previous study,[4] we reported a new chemosensor (**TDBQ**) based on diaza-18-crown-6 macrocycle appended with dual 7-hydroxyquinolines (7HQ) for recognition of Hg^{2+} ions to μM. As solved by X-ray structural analyses, **TDBQ** achieves Hg^{2+} recognition via the reduction of Hg^{2+}, forming a stoichiometric 2:1 Hg_2^{2+}/**TDBQ** complex in a 3D configuration. The above Hg_2^{2+}/**TDBQ** complex, though intriguing for its structural uniqueness, is not suited for further practical pursuit. The main disadvantage lies in the occurrence of complicated redox and stepwise recognition processes for the formation of a 2:1 Hg_2^{2+}/**TDBQ** complex. Furthermore, in a preliminary test, the binding constant as well as the fluorescence contrast may not be great enough to obtain high quality imaging for mercury recognition *in vitro*. Thus, as part of our continuous efforts, we then considered other latent pseudocryptands that are capable of providing compelling selectivity for mercury recognition.

To find high Hg^{2+}-ion specificity and/or association (sensitivity) in aqueous media, inspired by the framework of **TDBQ**, a potential candidate for synthesis and further examination is 8,8′-(1,4,10,13-tetrathia-7,16-diazacyclooctadecane-7,16-diyl)-bis(methylene)diquinolin-7-ol(**TTBQ**, Scheme 1(A)).

*To whom correspondence should be addressed. E-mail: meilin_ho@scu.edu.tw (M.-L. Ho), chop@ntu.edu.tw (P.-T. Chou).

(1) A few selected examples:(a) Huang, W.; Song, C.; He, C.; Lv, G.; Hu, X.; Zhu, X.; Duan, C. *Inorg. Chem.* **2009**, *48*, 5061–5072. (b) Wu, J.; Hwang, I.; Kim, K.; Kim, J. *Org. Lett.* **2007**, *9*, 907–910. (c) Che, Y.; Yang, X.; Zang, L. *Chem. Commun.* **2008**, 1413–1415. (d) Nolan, E. M.; Lippard, S. *J. Chem. Rev.* **2008**, *108*, 3443–3480. (e) Zhang, X.; Xiao, Y.; Qian, X. *Angew. Chem., Int. Ed.* **2008**, *47*, 8025–8029. (f) Pandey, S.; Azam, A.; Pandey, S.; Chawla, H. M. *Org. Biomol. Chem.* **2009**, *7*, 269–279.

(2) (a) Shi, W.; Ma, H. *Chem. Commun.* **2008**, 1856–1858. (b) Suresh, M.; Shrivastav, A.; Mishra, S.; Suresh, E.; Das, A. *Org. Lett.* **2008**, *10*, 3013–3016.

(3) For recent examples, see: (a) Yang, H.; Zhou, Z.; Huang, K.; Yu, M.; Li, F.; Yi, T.; Huang, C. *Org. Lett.* **2007**, *9*, 4729–4732. (b) Huang, J.; Xu, Y.; Qian, X. *J. Org. Chem.* **2009**, *74*, 2167–2170. (c) Chen, X.; Nam, S.-W.; Jou, M. J.; Kim, Y.; Kim, S.-J.; Park, S.; Yoon, J. *Org. Lett.* **2008**, *10*, 5235–5238. (d) Guliyev, R.; Coskun, A.; Akkaya, E. U. *J. Am. Chem. Soc.* **2009**, *131*, 9007–9013. (e) Wu, D. Y.; Huang, W.; Duan, C. Y.; Lin, Z. H.; Meng, Q. J. *Inorg. Chem.* **2007**, *46*, 1538–1540. (f) Wu, D. Y.; Huang, W.; Lin, Z. H.; Duan, C. Y.; He, C.; Wu, S.; Wang, D. H. *Inorg. Chem.* **2008**, *47*, 7190–7201. (g) Yoon, S.; Miller, E. W.; He, Q.; Do, P. H.; Chang, C. J. *Angew. Chem., Int. Ed.* **2007**, *46*, 6658–6661.

(4) Ho, M.-L.; Chen, K.-Y.; Wu, L.-C.; Shen, J.-Y.; Lee, G.-H.; Ko, M.-J.; Wang, C.-C.; Lee, J.-F.; Chou, P.-T. *Chem. Commun.* **2008**, 2438–2440.

Published on Web 10/09/2009

Scheme 1. (A) Synthetic Scheme of **TTBQ** and (B) Various Equilibrium Species of 7HQ in Aqueous Solution and Their Corresponding Absorption and Emission Maxima

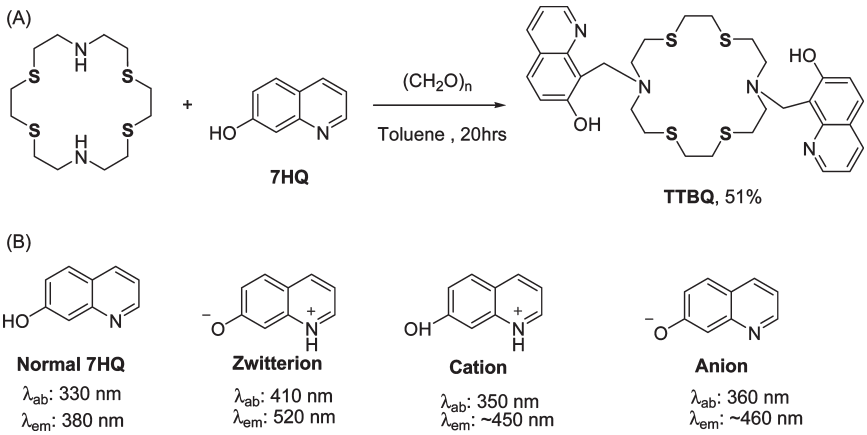

A semiempirical hard/soft, acid/base theory[5] simply implies that sulfur atoms are superior over oxygen containing receptors for binding Hg^{2+}. Moreover, the large atomic size of sulfur makes the tetrathiadiazacrown ether site (**TTBQ**) larger than that of the diaza-18-crown-6 ether (**TDBQ**) site. As a result, stoichiometric 2:1 Hg_2^{2+}:**TDBQ** binding may no longer be required for **TTBQ**. By forming a 1:1 Hg^{2+}:**TTBQ** complex, further quantitative analyses will be greatly simplified because the stepwise redox reaction occurring in **TDBQ** can be eliminated.

Also, inspired by the work by Farruggia et al.,[6] in the **TTBQ** architecture, we exploited phenolic and pyridyl nitrogen moieties, namely 7-hydroxyquinoline (7HQ), and attached it to each side arm of the diazacrown in order to enhance the complexation strength as well as to increase the solubility in aqueous solution. Moreover, due to the unique proton tautomerization, 7HQ in aqueous solutions, depending on pH, consists of four protropic equilibrium species: a neutral species (**Normal**), a **Cation**, an **Anion**, and a **Zwitterion**[7a] (see Scheme 1(B)). Upon metal ion binding, significant spectral variation is thus expected and should be suited for signal differentiation, i.e. signal transduction.

The following sections are organized in a sequence of steps, where we first unveil the synthetic route of **TTBQ**. Subsequently, studies of both photophysical and charge properties of **TTBQ** upon addition of Hg^{2+} are presented, followed by the structural determination of the **TTBQ**/Hg^{2+} complex via X-ray single crystal analysis. It is noteworthy that there are only a few examples of chemosensors for which the host/guest complexation can be directly probed by the associated crystal structures.[3c,4,8a,d] To gain further insight into the applicability, both the detection limit and selectivity of **TTBQ** will be discussed in detail. Finally, the capability of **TTBQ** for Hg^{2+} tracking *in vitro* is successfully demonstrated via fluorescence imaging.

2. Experimental Section

General Information and Materials. All solvents were distilled from appropriate drying agents prior to use. Commercially available reagents were used without further purification unless otherwise stated. All reactions were monitored by TLC with Macherey-Nagel precoated Glassic sheets (0.20 mm with fluorescent indicator UV254). Compounds were visualized with UV light at 254 and 365 nm. Flash column chromatography was carried out using silica gel from Merck (230−400 mesh). Infrared spectra were recorded on a Nicolet Magna II 550 FTIR apparatus with automatic background subtraction. ^{1}H NMR and ^{13}C NMR spectra were recorded on a Varian Unity 400 or Bruker Avance 400 spectrometer at 400 and 100 MHz, respectively. Chemical shifts (δ) are quoted in parts per million (ppm), and coupling constant (J) is recorded in Hertz (Hz). Low and high resolution mass spectra were recorded with a gas chromatograph−mass spectrometer (Finnigan MAT TSQ-46C GC/MS/MS/ DS).

8,8′-(1,4,10,13-Tetrathia-7,16-diazacyclooctadecane-7,16-diyl)-bis(methylene)diquinolin-7-ol (TTBQ). A solution of anhydrous toluene (50 mL), 1,4,10,13-tetrathia-7,16-diazacyclooctadecane[9] (124 mg, 0.38 mmol), 7-hydroxyquinoline (111 mg, 0.76 mmol), and paraformaldehyde (23 mg, 0.76 mmol) was refluxed for 20 h. The solvent was evaporated under reduced pressure, and residue was separated by chromatography on silica gel using MeOH/NH_4OH (4/1) as eluant to afford **TTBQ** (125 mg, 51%). ^{1}H NMR (400 MHz, $CDCl_3$, in ppm): δ 8.78 (dd, J_1 = 3.9 Hz, J_2 = 1.5 Hz, 2H), 8.05 (dd, J_1 = 7.9 Hz, J_2 = 1.5 Hz, 2H), 7.66 (d, J = 8.8 Hz, 2H), 7.23 (dd, J_1 = 7.9 Hz, J_2 = 3.9 Hz, 2H), 7.20 (d, J = 8.8 Hz, 2H), 4.59 (s, 4H), 2.96 (m, 8H), 2.88 (m, 8H), 2.79 (s, 8H). ^{13}C NMR (100 MHz, $CDCl_3$, in ppm): δ 159.18, 149.51, 147.65, 136.26, 128.36, 122.86, 119.90, 118.16, 113.63, 53.30, 51.75, 32.41, 29.56. MS (FAB) m/z 641 $(M+H)^+$. HRMS calcd for $C_{32}H_{41}O_2S_4N_4$ 641.2112, found 641.2104 (see the Supporting Information).

Preparation of TTBQ-Hg^{2+} Crystal. To the methanol solution (2 mL) of **TTBQ** (0.0056 g, mmol) was added the water solution (2 mL) of $Hg(ClO_4)_2$ (0.0040 g, mmole) in a 1:1 equivalent **TTBQ** and metal salt ratio at room temperature, giving a clear solution (pH = 7). Colorless crystals were obtained after standing for several days in ca. 30% yield. Anal. Calc. for $C_{32}H_{46}Cl_4HgN_4O_{20}S_4$: C 30.09, H 3.63, N 4.39; Found: C 30.07, H 3.61, N 4.37. IR (KBr) ν (cm^{-1}): 3009 (m), 2908 (m), 2809 (m), 1614 (vs), 1508 (s), 1475 (m), 1436 (s),

(5) Pearson, R. G. *J. Am. Chem. Soc.* **1963**, *85*, 3533–3539.
(6) Farruggia, G.; Iotti, S.; Prodi, L.; Montalti, M.; Zaccheroni, N.; Savage, P. B.; Trapani, V.; Sale, P.; Wolf, F. I. *J. Am. Chem. Soc.* **2006**, *128*, 344–350.
(7) (a) Mason, S. F.; Philp, J.; Smith, B. E. *J. Chem. Soc. A* **1968**, 3051–3056. (b) Angulo, G.; Organero, J. A.; Carranza, M. A.; Douhal, A. *J. Phys. Chem. B* **2006**, *110*, 24231–24237. (c) Manca, C.; Tanner, C.; Leutwyler, S. *Int. Rev. Phys. Chem.* **2005**, *24*, 457–488. (d) Lee, S.-I.; Jang, D.-J. *J. Phys. Chem.* **1995**, *99*, 7537–7541.
(8) (a) Zhao, Y.; Lin, Z.; He, C.; Wu, H.; Duan, C. *Inorg. Chem.* **2006**, *45*, 10013–10015. (b) Dhir, A.; Bhalla, V.; Kumar, M. *Org. Lett.* **2008**, *9*, 4891–4894. (c) Wu, D.; Huang, W.; Lin, Z.; Duan, C.; He, C.; Wu, S.; Wang, D. *Inorg. Chem.* **2008**, *47*, 7190–7201. (d) Wu, D.; Huang, W.; Duan, C.; Lin, Z.; Meng, Q. *Inorg. Chem.* **2007**, *46*, 1538–1540.
(9) Black, D. St. C.; Mclean, I. A. *Chem. Commun.* **1968**, 1004–1006.

Table 1. Crystal Data for **TTBQ** and **TTBQ-Hg^{2+}**

	TTBQ	TTBQ-Hg^{2+}
empirical formula	$C_{32}H_{40}N_4O_2S_4$	$C_{32}H_{46}C_{l4}HgN_4O_{20}S_4$
formula weight	640.92	1277.36
temperature (K)	295(2)	150(2)
wavelength	0.71073 Å	0.71073 Å
crystal system	triclinic	monoclinic
space group	$P\bar{1}$	$C2/c$
a (Å)	8.8095(5)	21.2169(4)
b (Å)	11.6885(7)	10.8426(2)
c (Å)	17.0124(10)	17.7090(3)
α (°)	93.617(1)	90
β (°)	101.032(1)	119.1335(7)
γ (°)	108.264(1)	90
volume (Å^3)	1618.48(16)	4397.09(13)
Z	2	4
density (calculated)	1.315 Mg/m^3	1.930 Mg/m^3
absorption coefficient (mm^{-1})	0.329	4.018
F(000)	680	2552
crystal size	0.50 × 0.20 × 0.20 mm^3	0.45 × 0.35 × 0.10 mm^3
theta range for data collection	1.23 to 25.00°.	1.78 to 27.50°.
index ranges	$-10 \le h \le 10$,$-13 \le k \le 13$,$-20 \le l \le 20$	$-30 \le h \le 34$,$-11 \le k \le 14$,$-22 \le l \le 19$
reflections collected	17739	12950
independent reflections	5707 [R(int) = 0.0424]	5006 [R(int) = 0.0602]
completeness to theta = 25.00°	100.0%	99.2%
absorption correction	semiempirical from equivalents	semiempirical from equivalents
refinement method	full-matrix least-squares on F^2	full-matrix least-squares on F^2
data/restraints/parameters	5707/0/381	5006/0/314
goodness-of-fit on F^2	1.004	1.087
final R indices [$I > 2\sigma(I)$][a]	R1 = 0.0787, wR2 = 0.2151	R1 = 0.0360, wR2 = 0.0898
R indices (all data)	R1 = 0.1146, wR2 = 0.2442	R1 = 0.0418, wR2 = 0.0926
largest diff. peak and hole	1.210 and −0.365 e.Å^{-3}	0.872 and −1.301 e.Å^{-3}

[a] $R(F) = \Sigma||F_o| - |F_c||/\Sigma|F_o|$ and $wR(F^2) = [\Sigma w|F_o^2 - F_c^2|^2/\Sigma w(F_o^4)]^{1/2}$.

1349 (m), 1311 (s), 1274 (s), 1205 (s), 1158 (m), 1129 (s), 1091 (m), 1021 (m), 981 (m), 785 (m), 755 (m), 712 (w).

Crystallographic Data Collection and Refinement. The chosen crystals of **TTBQ** and **TTBQ-Hg^{2+}** crystal were both mounted on a glass fiber. Data collections were carried out on a Siemens SMART diffractometer with a CCD detector with Mo radiation (λ = 0.71073 Å) at 150 K. A preliminary orientation matrix and unit cell parameters were determined from 3 runs of 15 frames each, with each frame corresponding to a 0.3° scan in 10 s, followed by spot integration and least-squares refinement. For each structure, data were measured using ω scans of 0.3° per frame for 20 s until a complete hemisphere had been collected. Cell parameters were retrieved using SMART[10] software and refined with SAINT[11] on all observed reflections. Data reduction was performed with the SAINT[11] software and corrected for Lorentz and polarization effects. Absorption corrections were applied with the program SADABS.[12] Direct phase determination and subsequent difference Fourier map synthesis yielded the positions of all non-hydrogen atoms, which were subjected to anisotropic refinements. All hydrogen atoms were fixed at calculated positions and refined using a riding mode. The final full-matrix, least-squares refinement on F^2 was applied for all observed reflections [$I > 2\sigma(I)$]. All calculations were performed with the SHELXTL-PC V 6.12 software package.[13] Crystallographic data and experimental details of refinements for structural analyses are given in Table 1.

(10) *SMART V 4.043 Software for CCD Detector System*; Siemens Analytical Instruments Division: Madison, WI, 1995.

(11) *SAINT V 4.035 Software for CCD Detector System*; Siemens Analytical Instruments Division: Madison, WI, 1995.

(12) Sheldrick, G. M. *Program for the Refinement of Crystal Structures*; University of Göttingen: Göttingen, Germany, 1993.

(13) SHELXTL 6.12 (PC-Version). *Program Library for Structure Solution and Molecular Graphics*; Siemens Analytical Instruments Division: Madison, WI, 2000.

Crystallographic data (excluding structure factors) of **TTBQ** and **TTBQ-Hg^{2+}** crystal for the structures reported in this paper have been deposited with the Cambridge Crystallographic Data Centre as supplementary publications Nos. CCDC 749836 and CCDC 749837. Copies of the data can be obtained free of charge on application to CCDC, 12 Union Road, Cambridge CB21EZ, UK (fax: (+44) 1223−336−033; e-mail: deposit@ccdc.cam.ac.uk).

UV−vis and Fluorescence Titration of Compounds TTBQ with Hg^{2+} Ions. The solution of compound **TTBQ** (1.50×10^{-6} M) was prepared by using spectroscopic grade MeOH-H_2O (1:10, v/v). The stock solution of Hg^{2+} ions (1×10^{-2} M) was prepared by using mercury(II) perchlorate hydrate dissolved in H_2O. In titration experiments, a 3.0 mL solution of **TTBQ** (1.50×10^{-6} M) was filled in a quartz optical cell of 1 cm optical path length, and the Hg^{2+} stock solution was added gradually into the quartz cell with a micropipet. The absorption and emission spectra of **TTBQ** in a quartz cell were recorded at 298 K.

Derivation of Association Constant. The association constant K_a of the **TTBQ** + Hg^{2+} complex formation can be deduced via the relationship of absorbance, A, versus added Hg^{2+} concentration (C_g), expressed in eq 1 (see also the Supporting Information for detailed derivation), and calculated by the UV−vis absorption method as follows

$$\begin{array}{lccc} & \textbf{TTBQ} & + Hg^{2+} \rightleftharpoons & \textbf{TTBQ}/Hg^{2+} \\ \text{initial} & C_0 & C_g & 0 \\ \text{final} & C_M & \sim C_g & C_p \end{array}$$

$$\therefore \frac{A_0}{A_0 - A} = \frac{\varepsilon_M(K_a C_g + 1)}{(\varepsilon_M - \varepsilon_p)(K_a C_g)} = \left(\frac{\varepsilon_M}{\varepsilon_M - \varepsilon_p}\right)\left[\frac{1}{K_a C_g} + 1\right] \quad (1)$$

where C_g is the added guest (Hg^{2+}) concentration, and A_0 (ε_M) and A (ε_P) denote the absorbance (molar extinction coefficient) of free **TTBQ** and solution after adding Hg^{2+}, respectively, at 352 nm.

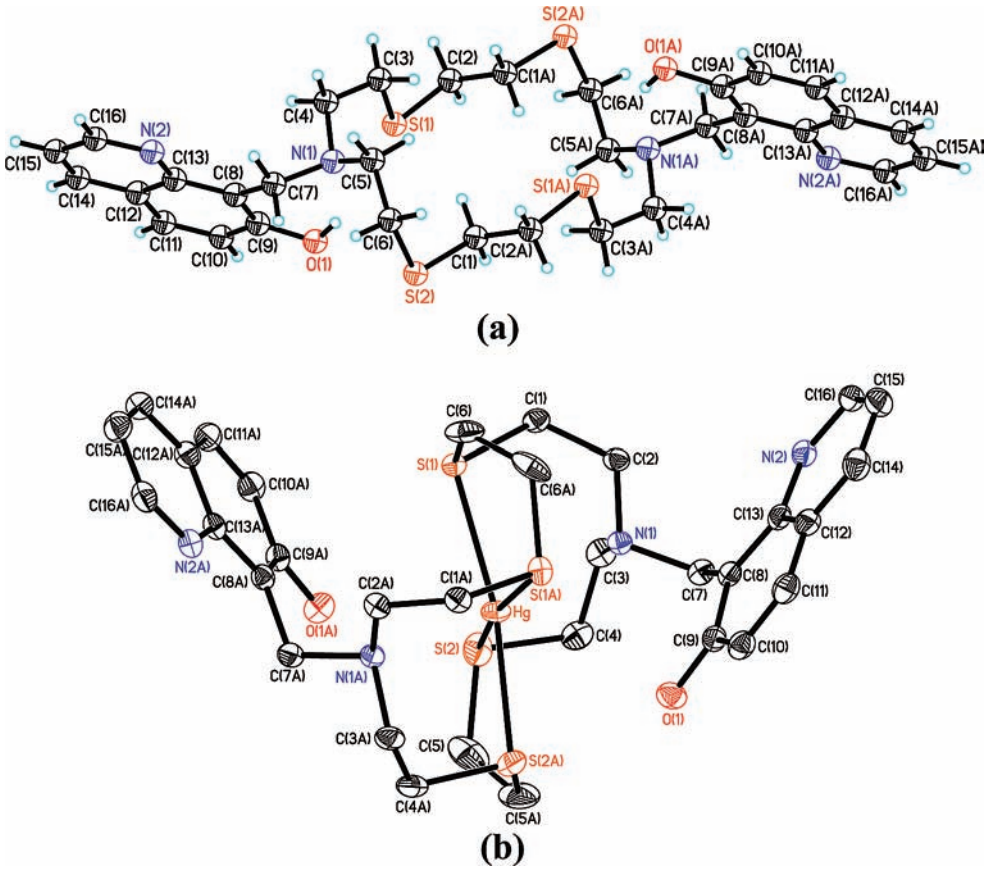

Figure 1. ORTEP diagrams of (a) **TTBQ** and (b) **TTBQ** + Hg^{2+} with thermal ellipsoids shown at the 30% probability level. Selected bond lengths (Å) and bond angles (°) of **TTBQ** + Hg^{2+}: Hg−S(1) 2.6314(9), Hg−S(2) 2.641(1), Hg−S(1A) 2.6314(9), Hg−S(2A) 2.641(1), Hg−N(1A) 2.758(3), Hg−N(1) 2.758(3), Hg−O(1) 3.388(3), Hg−O(1A) 3.388(3), S(1A)−Hg−S(1) 83.43(4), S(1A)−Hg−S(2) 169.85(3), S(1)−Hg−S(2) 98.09(4), S(1A)−Hg−S(2A) 98.09(4), S(1)−Hg−S(2A) 169.84(3), S(2)−Hg−S(2A) 82.19(5).

X-ray Absorption Spectroscopy. The X-ray absorption experiments were carried out at the National Synchrotron Radiation Research Center (NSRRC), Hsinchu, Taiwan. All spectra of the Hg L_{III}-edge were recorded at room temperature at the wiggler beamline 17C with a double Si(111)-crystal monochromator. The energy resolution $\triangle E/E$ is 2×10^{-4}. High harmonics were removed by Rh-coated mirrors. X-ray absorption near the edge structure (XANES) spectrum of **TTBQ**-mercury crystal was recorded in fluorescence mode. The spectra of reference compounds, $HgCl_2$ and Hg_2Cl_2, were recorded in transmission mode. Energy calibration of all spectra was based on $HgCl_2$ at 12284.1 eV.[14] $HgCl_2$ and Hg_2Cl_2 were purchased from Sigma-Aldrich.

Preparation and Staining of Cell Cultures. HEK 293T cells were cultured in Dulbecco's modified eagle medium (DMEM, Invitrogen, Carlsbad, CA) supplemented with 10% fetal bovine serum (FBS, Invitrogen) and glutamine (2 mM). One day before imaging, cells were passed and plated on 18-mm glass coverslips coated with poly-Lysine (50 μg/mL, Sigma, St. Louis, MO). Immediately before the experiments, cells were washed with DMEM, incubated with the probe (1.0 μM) in DMEM for 60 min at 37 °C, washed with PBS, and imaged. Experiments to assess Hg^{2+} uptake were performed in the same media supplemented with 40 μM of Hg^{2+} for 10 min at 37 °C.

Cellular Toxicity from Cell Proliferation Test. The cellular toxicity of **TTBQ** loaded HEK 293T cells was evaluated by using a colorimetric assay agent, 3-(4,5-dimethylthiazol-2-yl)-2,5-diphenyltetrazolium bromide (MTT) (Roche, Mannheim, Germany). HEK 293T was seeded in a 24 well plate with 5×10^4 cells per well and allowed to grow overnight before compound feeding. Five different dosages were given, in addition to the control group, to reach final concentrations of 0.90, 1.77, 3.46, 6.61, and 12.11 μM. After 24 h of incubation, each well was washed with phosphate buffer saline (PBS: 137 mM NaCl, 2.68 mM KCl, 10 mM Na_2HPO_4, 1.76 mM KH_2PO_4, pH 7.4) three times and replenished with 500 μL of culturing medium with 10% MTT agent. After 30 min of incubation and medium removal, the newly formed purple MTT-formazan was dissolved in 200 μL of dimethyl sulfoxide (Sigma), and the absorbance was measured at 570 nm by a spectrophotometer (Tecan Infinite F200). A total of 4 trials were performed for the assurance of reproducibility.

Fluorescence Imaging Experiments. Imaging experiments were performed with a Zeiss LSM 710 Confocal Spectral Inverted Microscope Imaging System and a 25× objective lens. Cells were immersed in PBS during the imaging process to avoid background fluorescence caused by the culture medium. Excitation of **TTBQ**-loaded cells at 351 nm was carried out with an Ar−UV laser, and emission was collected in a window from 420 to 780 nm. **TTBQ** (1 μM) was incubated with live cell samples for 60 min at 37 °C. To obtain the fluorescence spectra in the range of 420 to 780 nm, internal PMTs were used to collect the signals in an 8 bit unsigned 512 × 512 pixels at 400 Hz scan speed.

2. Results and Discussion

Synthesis and Structure of TTBQ. TTBQ was afforded in ~50% yield via a Mannich type of condensation, a facile process of refluxing 1,4,10,13-tetrathia-7,16-diazacyclooctadecane with 7-HQ in the presence of

(14) Bernaus, A.; Gaona, X.; Ivask, A.; Kahru, A.; Valiente, M. *Anal. Bioanal. Chem.* **2005**, *382*, 1541–1548.

paraformaldehyde in toluene for 20 h (see Scheme 1 and the Supporting Information). The structure of the **TTBQ** was identified by ^{1}H NMR, ^{13}C NMR, MS, and X-ray diffractometer methods (see also the Supporting Information). The X-ray structure of **TTBQ** shown in Figure 1(a) reveals an open cagelike geometric conformation due to a strong intramolecular O(1)−H(1)---N(1) hydrogen bond with an O(1)---N(1) distance of 2.7498 Å originating from 7HQ and the macrocycle ring. Two 7HQ fragments are located oppositely and perpendicular to the macrocycle ring, with a dihedral angle of approximately 68° between 7HQ and the least-squared plane of the macrocycle ring (see TOC and Figure 1(a)).

Spectroscopic and Structural Properties of TTBQ with Hg^{2+}. As shown in Figure 2, the UV−vis spectrum of **TTBQ** in MeOH/H_2O (1:10) (pH = 7, black line) is characterized by two lower lying absorption bands maximized at 327 and 403 nm, which are reasonably assigned to the **Normal** and **Zwitterion** species of 7HQ chromophore, respectively, in neutral water (see Scheme 1 for the notation).[7b−d] Upon addition of Hg^{2+}, the absorbance at 403 nm tends to decrease, accompanied by a gradual increase of a new blue-shifted band at 352 nm. This new blue-shifted band at 352 nm is a characteristic of the **Anion** species.[7d] During the Hg^{2+} titration it should be noted that there appears an intersection at 384 nm. Since the equilibrium involves **Normal**, **Zwitterion**, and **Anion** forms (see Scheme 1), it is rare to have an isosbestic point among three species. The result can be rationalized by negligible absorption extinction coefficient at 384 nm for the **Normal** species, making virtually a pseudoisosbestic point between **Anion** and **Zwitterion** during the titration.

The binding stoichiometry between **TTBQ** and Hg^{2+} was then determined from Job's plot evaluation. Accordingly, the increase of absorption at 352 nm was plotted against the mole fraction of Hg^{2+} under a constant concentration of [**TTBQ**] + [Hg^{2+}] = 1.50 μM. The result of Job's plot shown in Figure S5 (see the Supporting Information) clearly indicates a 1:1 complex formation between **TTBQ** and Hg^{2+}. Based on a 1:1 stoichiometry, the binding constant of complexation can thus be deduced via the relationship of absorbance, A, versus added Hg^{2+} concentration (C_g) expressed in eq 1 (see the Experimental Section). A straight line plot of $A_0/(A_0-A_{352\ nm})$ versus $1/C_g$ (see Figure S6) reconfirms the 1:1 binding of Hg^{2+} for the complexation. Accordingly, K_a can be deduced to be 13,020 ± 520 M^{-1} from the quotient of intercept divided by the slope.

The results elaborated above show distinctly different binding stoichiometry between **TTBQ**/Hg^{2+} (1:1) and **TDBQ**:Hg_2^{2+} (1:2). To gain more insight into the structural/stoichiometry relationship, crystallization of the **TTBQ**/Hg^{2+} complex was then carried out from 1:1 mixture of **TTBQ** and $Hg(ClO_4)_2 \cdot xH_2O$. The X-ray determination of the single crystal directly evidence the formation of the $[Hg(H_2TTBQ)]^{4+}$ complex with a 1:1 Hg^{2+}:**TTBQ** ratio. As shown in Figure 1(b), the molecular structure of $[Hg(H_2TTBQ)]^{4+}$ reveals the configuration of **TTBQ** ligand coordinated Hg^{2+} ion, in which an Hg^{2+} ion is trapped into the macrocycle ring, mainly due to the coordination of Hg^{2+} ion with four sulfur atoms (S1, S2, S(1A), S(2A), with Hg−S(1) and Hg−S(2) bond lengths of 2.6314(9) and 2.641(1) Å, respectively.

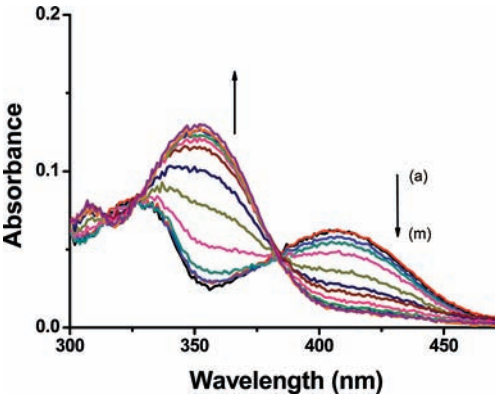

Figure 2. Absorption spectrum changes of **TTBQ** (1.5 μM) upon addition of various concentrations of anhydrous Hg^{2+} in aqueous solution at (a) 0, (b) 4.0×10^{-5}, (c) 5.3×10^{-5}, (d) 6.7×10^{-5}, (e) 8.0×10^{-5}, (f) 9.3×10^{-5}, (g) 1.1×10^{-4}, (h) 1.2×10^{-4}, (i) 1.3×10^{-4}, (j) 1.5×10^{-4}, (k) 1.6×10^{-4}, (l) 1.7×10^{-4}, and (m) 1.8×10^{-4} M. (black) absorption spectrum of **TTBQ** in aqueous solution.

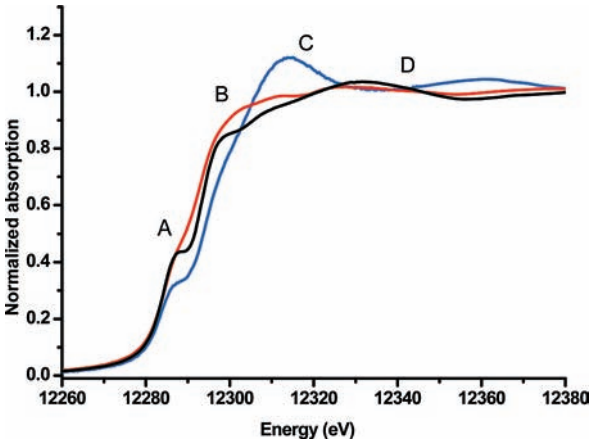

Figure 3. Normalized XANES spectra for **TTBQ**-mercury crystal (blue), $HgCl_2$ (black), and Hg_2Cl_2 (red).

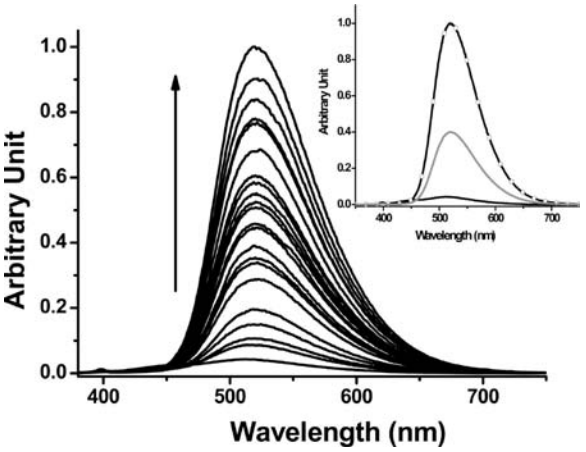

Figure 4. The emission spectra of **TTBQ** (1.5 μM in aerated aqueous solution) upon addition of Hg^{2+} in an increment of 13.3 μM. λ_{ex} = 352 nm. Insert: The emission spectra of **TTBQ** (1.5 μm, black) in the presence of 280 μM of Hg^{2+} (-○-) and the addition of 0.1 mM DMPS (gray). λ_{ex} = 355 nm.

Two nitrogen atoms (N(1) and N(1A)) of the macrocycle ring are weakly bonded to the Hg^{2+} ion, with a longer Hg−N bond distance of 2.758(3) Å. Two 7HQ fragments are no

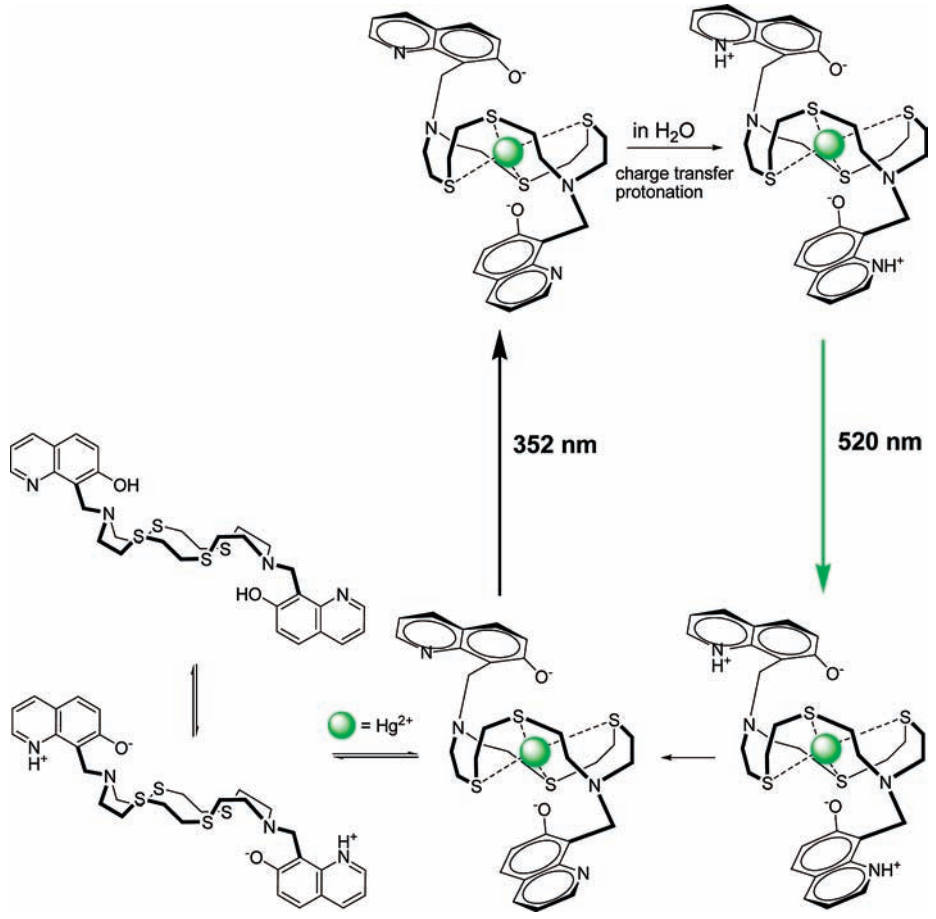

Figure 5. Proposed mechanism of **TTBQ** with Hg^{2+} in neutral aqueous solution.

longer perpendicular to the macrocycle ring but have moved closer to it, with a smaller dihedral angle of 44.8° between 7HQ and the squared plane of the macrocycle ring. This configuration is distinctly different from that of the **TDBQ**:Hg_2^{2+} complex.[4] As evidenced by the Hg−O(1) (of 7HQ in **TTBQ**, see Figure (1b) and TOC) distance of 3.388(3) Å, the result may be rationalized by the existence of weak Hg^{2+}-O(1) interaction, which pulls the two 7HQ moieties inward and closer to the macrocycle ring. As a result, the **TTBQ**-Hg^{2+} complex reveals a cagelike geometry, in which the macrocycle ring is virtually capped by two 7HQ chromophores. In other words, under the driving force of Hg^{2+} recognition, thermodynamically, one can envisage that **TTBQ** has been reshaped into a 3D-like structure, in which the dual 7HQ functions as sheathlike plugs to accommodate Hg^{2+}.

We then performed XANES measurement at the Hg L_{III}-edge. Our goal in this approach is to provide further evidence of the charge of the mercury ion in the as-prepared single crystal upon recognition. The results are compiled in Figure 3. For comparison, spectra of $HgCl_2$ and Hg_2Cl_2 are also shown in Figure 3. According to the electric-dipole selection rules, the spectral features in the region of 12280−12295 eV result from the transition of $2p_{3/2} \rightarrow 6s$,[15] while those of > 12295 eV are attributed to the transitions of $2p_{3/2} \rightarrow 6d$ of the Hg(I) and Hg(II).

(15) Studer, F.; Pelloquin, D.; Maignan, A.; Michel, C.; Hervieu, M.; Raveau, B. *Physica C* **1995**, *242*, 1–11.

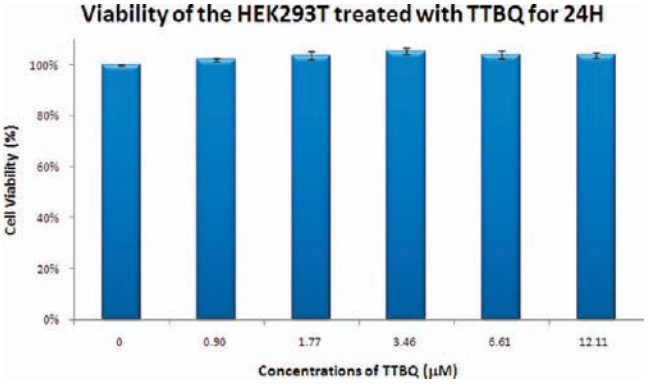

Figure 6. MTT assay for the viability of HEK 293T treated with various concentrations of **TTBQ** for 24H. Note that the cells remained nearly 100% viable in all tested groups, even up to 12.11 μM. Error bars represent the standard deviations of 4 trials.

Moreover, Hg^{2+} exhibits a distinct shoulder at 12285 eV due to the high density of the empty 6s electronic state. Evidently, the XANES spectrum of the single crystal shown in Figure 3 indicates that the oxidation state of mercury ion is best described as Hg^{2+}, consistent with the X-ray crystal analysis.

As for the fluorescent detection of Hg^{2+} in aqueous solution, upon excitation at e.g. 352 nm, the free **TTBQ** exhibits a broad, weak emission band, which could be attributed to the overlap of **Anion** (459 nm) and **Zwitterion** (~520 nm) emission. Upon addition of Hg^{2+}, under

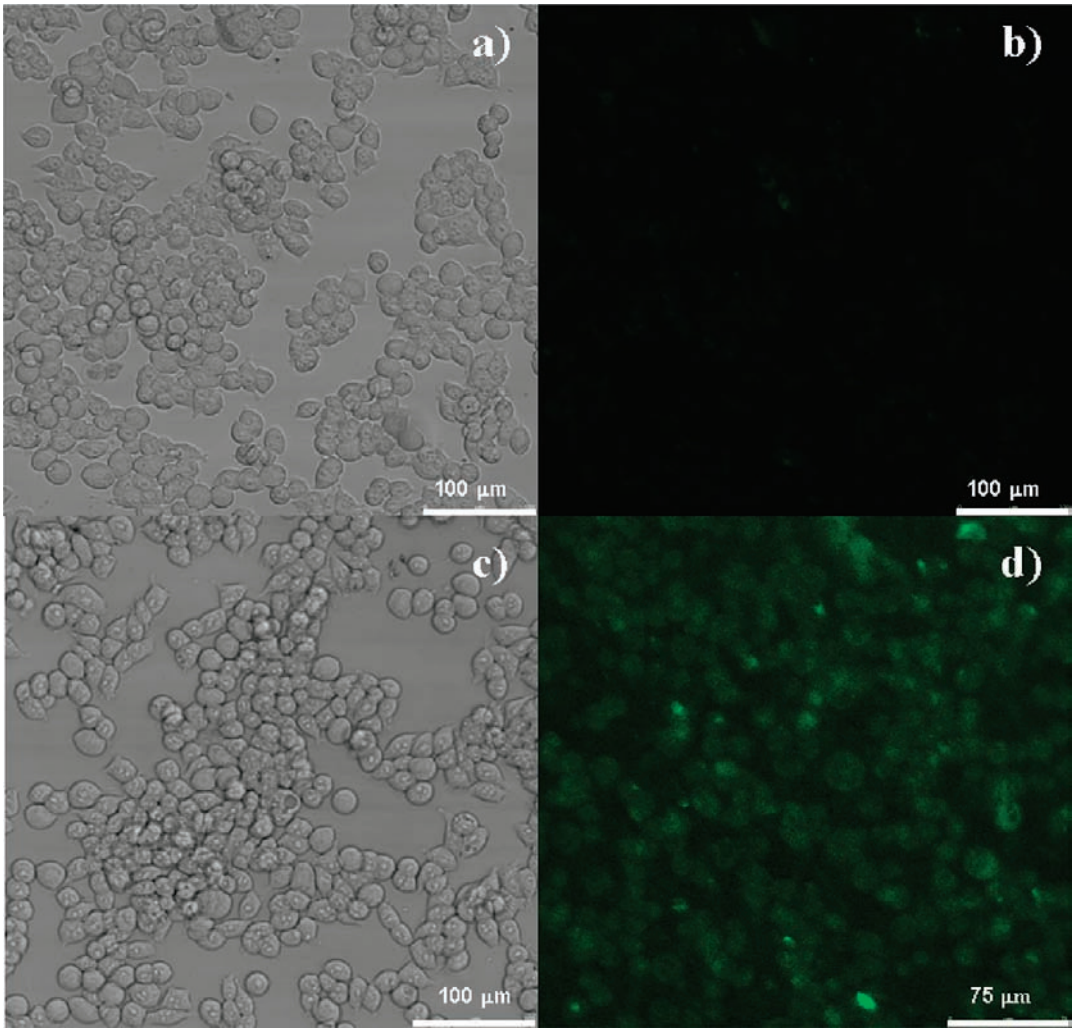

Figure 7. (a) Bright-field image of cells. Scale bar = 100 μm. (b) Confocal fluorescence image of live HEK 293T cells incubated with 1 μM **TTBQ** for 60 min at 37 °C. Scale bar = 100 μm. (c) Bright-field image of **TTBQ** loaded cells exposed to 40 μM of Hg^{2+} for 10 min at 37 °C. (d) Confocal fluorescence image of live HEK 293T cells incubated with **TTBQ** loaded cells exposed to 40 μM of Hg^{2+} at 37 °C, confirming their viability. Scale bar = 75 μM.

similar 352 nm excitation, which is the peak wavelength of the **TTBQ Anion** species upon incorporating Hg^{2+}, a unique emission maximized at 520 nm is observed. Owing to the similarity in spectral features, the emission can unambiguously be assigned to a **Zwitterion** origin. After reaching the end point of Hg^{2+} titration, the 520 nm emission renders a 25-fold increase in intensity relative to that of the free **TTBQ** (see Figure 4). For rationalization, evidenced by the **Anion** formation, the incorporation of Hg^{2+} must deprotonate from the 7HQ moiety by forming Hg^{2+}-O^{-}(1) ionic interaction (vide infra). We thus propose that the **Anion** species, upon excitation, then undergoes excited-state charge transfer from phenolic (HOMO) to the pyridyl (LUMO) moiety in aqueous solution. This net result, depicted in Figure 5, resembles a **Zwitterion**-like configuration of 7HQ in the excited state,[16] giving rise to an intense 520 nm **Zwitterion** emission. Also, the rigidity of the overall 3D-complexation structure may also play a role in the leap in emission intensity.

Reversibility, Selectivity, and pH Investigation of the Hg^{2+} Detection System. A key requirement of ideal chemosensor function is that guest binding must occur reversibly.[17] Based on the fluorescence spectrum, the reversibility of the recognition process of **TTBQ** toward Hg^{2+} was tested by adding a mercury chelating agent, sodium-2,3-dimercapto-1-propanesulfonate (DMPS). As shown in the insert of Figure 4, after addition of 0.1 mM DMPS into the solution containing **TTBQ** (1.5 μM) and Hg^{2+} (280 μM), 60% of the **Zwitterion** emission intensity was quenched. Thus, the reversible response of **TTBQ** to Hg^{2+} indicates that **TTBQ** is a chemosensor rather than a chemodosimeter for Hg^{2+}.

To examine the selectivity of the chemosensor, the fluorescence responses of **TTBQ** to other metal ions were carried out. **TTBQ** (1.5 μM solution) was then tested in the presence of other metal cations, including alkali- and alkaline-earth metal ions, such as Li^{+}, Na^{+}, K^{+}, Mg^{2+}, Ca^{2+} (1 mM) and first-row transition-metal ions Fe^{2+}, Cu^{2+} (250 μM) and 300 μM for other cations, such as Zn^{2+}, $Pb^{2+,}$ and Al^{3+}. As shown by the enhancement of emission intensity after adding 0.5 mM Hg^{2+} with respect to the competing metal ions (Figure S7), **TTBQ** has distinctly leaping fluorescence intensity upon recognizing

(16) Chou, P.-T.; Wei, C.-Y.; Wang, C.-R. C.; Hung, F.-T.; Chang, C.-P. *J. Phys. Chem. A* **1999**, *103*, 1939–1949.

(17) Bell, T. W.; Hext, N. M. *Chem. Soc. Rev.* **2004**, *33*, 589–598.

Hg^{2+}, while other ions induce much smaller fluorescence increments. This experiment confirms the noteworthy selectivity of **TTBQ** for Hg^{2+}.

The proper pH condition was subsequently evaluated for the biological applicability upon application as a chemosensor. The ratio of fluorescence intensity of **TTBQ** at various pH values in the absence and presence of the Hg^{2+} in aqueous solution ($MeOH:H_2O$ 1:10) is shown in Figure S8. The results clearly indicate that **TTBQ** can respond to Hg^{2+} in the pH range of 5.5 to 7.5, with the fluorescence intensity varying less than 10%, whereas in this region, the free **TTBQ** has much weaker fluorescence, suggesting that **TTBQ** is suitable for application under physiological conditions.

Fluorescence Sensing *in Vitro*. Prior to cell imaging, the cellular toxicity of **TTBQ** has to be examined, which was tested based on cell proliferation in this study. Taking advantage of easy handling, HEK 293T cells were employed as a model for the *in vitro* experiment. In this approach, the cell viabilities after incubation with various concentrations of **TTBQ** were measured using MTT (3-(4,5-dimethylthiazol-2-yl)-2,5-diphenyltetrazolium bromide) assay. The results depicted in Figure 6 clearly indicate that cells incubated with up to 12.11 μM of **TTBQ** remained almost 100% viable after 24 h of feeding time. The biocompatibility demonstrated here was quiet satisfying as the cells survived in the highest concentration evaluated, which was about 12 times of the working dosage required to achieve discernible sensing.

We then explored the capability of **TTBQ** to coordinate with Hg^{2+} in living cells. Confocal microscopy images of live HEK 293T cells loaded with 1 μM of **TTBQ** for up to 60 min at 37 °C show nearly dark background intracellular fluorescence (see Figure 7b and the Table of Contents graphic). In sharp contrast, **TTBQ**-labeled cells exposed to 40 μM of Hg^{2+} for 10 min at 37 °C show greatly enhanced intracellular fluorescence (Figure 7d and the Table of Contents graphic). Bright-field measurement confirms that the cells were viable, with intact morphology, throughout the imaging studies (Figure 7a,b).

3. Conclusion

To sum up, several conclusions can be drawn from this study: (1) **TTBQ** has been strategically designed and synthesized via a facile Mannich type of reaction. The 3D-complexation site with sulfur coordination makes **TTBQ** an exquisite case in point for Hg^{2+} selective recognition. The detection limit could be in the sub-μM concentration range for Hg^{2+} ions in aqueous solution. (2) Single crystals of both **TTBQ** and the **TTBQ**-Hg^{2+} complex have been unambiguously resolved, with the latter possessing a Hg center trapped into the thioazacrown with a 3D-complexation. This cagelike behavior is accompanied by 25-fold luminescence enhancement upon Hg^{2+} addition. Moreover, the two 7HQ moieties not only act as sheathing attached to diaza-18-thiocrown-6, forming dual plugs and greatly enhancing the binding strength with Hg^{2+}, but also serve as a signal transducer. (3) For practical application, the recognition ability and biocompatibility of **TTBQ** have been successfully demonstrated *in vitro* using HEK 293T cells with confocal microscopy. The significance of this study lies in the 3D 1:1 (in molar ratio) host/guest type of recognition in aqueous solution, which is different from the much complicated 1:2 (in molar ratio) host/guest type of recognition that we previously published in *Chem. Commun.*[4] Moreover, using **TTBQ** as a host, we exemplify a model to trap Hg^{2+} via a combination of 3D-complexation structure, hard/soft, hydrogen bonding, and weak ionic interaction. The strategy can be greatly expanded to other **TTBQ** analogues, for which the recognition site is designed to possess a 3D structure with a more hydrophobic environment, such that the bulk water can be excluded to increase the affinity. An ultimate goal will be aimed at mimicking the enzymatic system to optimize both sensitivity and selectivity. Accordingly, it is clear that future extension of this type of chemosensors should be versatile and perspective.

Acknowledgment. This research was supported by a grant (NSC98-2113-M-031-001-MY2) from the National Science Council, Taiwan.

Supporting Information Available: Figures s1−s8 and cif files. This material is available free of charge via the Internet at http://pubs.acs.org.